ELSEVIER

Contents lists available at ScienceDirect

Medical Engineering and Physics

journal homepage: www.elsevier.com/locate/medengphy



Check for updates

Study of Tissue Damage Induced by Insertion of Composite-Coated Needle

Kavi Patel, Parsaoran Hutapea

Department of Mechanical Engineering, Temple University, Philadelphia, PA 19122, United States of America

ARTICLE INFO

Keywords: Needle coating Insertion force reduction Minimization of tissue-damage

ABSTRACT

Medical interventions have significantly progressed in developing minimally invasive techniques like percutaneous procedures. These procedures include biopsy and internal radiation therapy, where a needle or needle-like medical device is inserted through the skin to access a target inside the body. Ensuring accurate needle insertion and minimizing tissue-damage or cracks are critical in these procedures. This research aims to examine the coated needle effect on the force required to insert the needle (i.e., insertion force) and on tissue-damage during needle insertion into the bovine kidney. Reducing the needle insertion force, which is influenced by needle surface friction, generally results in a reduction in tissue-damage. Surgical needles were coated with a composite material, combining Polytetrafluoroethylene, Polydopamine, and Activated Carbon. Force measurement during needle insertion and a histological study to determine tissue-damage were conducted to evaluate the effectiveness of the coating. The insertion force was reduced by 49 % in the case of the coated needles. Furthermore, a histological analysis comparing tissue-damage resulting from coated and uncoated needles revealed an average 39 % reduction in tissue-damage with the use of coated needles. The results of this study demonstrate the potential of coated needles to enhance needle insertion and safety during percutaneous procedures.

1. Introduction

Certain surgical procedures, such as biopsies, internal radiation therapy, and thermal ablation necessitate the utilization of surgical needles [1–3]. During these procedures, medical professionals insert the needle or needle-like structure through the outside skin and guide it to a specific internal tissue location or target. A force required to insert the needle can be considered as an insertion force. The insertion force is determined by the friction between the needle and the tissue during insertion, which can cause tissue-damage. A number of research findings propose that lowering the force required for needle insertion minimizes tissue-damage and potentially improves the precision of the insertion [4–8]. Various strategies, including adjusting the needle insertion speed [9,10], modifying the needle design [4-6,10-13], applying coatings to the needle surface [14-18], and employing different insertion techniques [19], have been previously employed to reduce the insertion force. Among these, applying a coating to the needle surface serves the dual purpose of enhancing its surface properties and preserving its original design and geometry, which are essential for numerous surgical interventions.

The main goal of the needle coating is to lower the needle surface friction, which decreases the insertion force during needle insertion

inside the tissue. Polydopamine (PDA) was chosen for its exceptional adhesion properties to both organic and inorganic surfaces, as well as its biocompatibility and biodegradability [18]. Polytetrafluoroethylene (PTFE), on the other hand, was selected due to its low coefficient of friction, antimicrobial properties, hydrophobic nature, biocompatibility, and resistance to chemicals and drugs [18]. PTFE is known for its non-stick property, which can compromise the durability of the coating. To overcome this limitation, PDA was incorporated into the composite to enhance its overall durability. In addition, activated carbon (AC) was included as a filler in the composite coating. Its primary function is reinforcing PTFE surface cracks and irregularities, ensuring a smoother and more even coating [18]. Activated Carbon (AC) stands out due to its nontoxic properties, remarkable biocompatibility, and hemocompatibility, marking it as a versatile material. Its versatility becomes apparent in its wide array of applications across various industries, including cosmetics and the medical field [20]. Its benefits encompass not only dental care [21], skin care [22], and oral medications [23] but also extend to blood perfusion, a technique utilizing an activated carbon-coated column to filter blood from toxins [24]. In addition, the biodegradability of activated carbon (AC) is fundamentally non-viable due to its inert carbonaceous composition and the absence of mechanisms for enzymatic or microbial decomposition [25].

E-mail address: hutapea@temple.edu (P. Hutapea).

^{*} Corresponding author.

Histological analysis serves as a valuable tool for understanding tissue structure and detecting any abnormalities [5,6,26]. Sahlabadi [5] developed a honeybee-inspired needle and found that their needle helped in reducing tissue-damage by 31 %. Similarly, Gidde [6] used a mosquito-inspired needle and observed a reduction in tissue-damage by 27 %. Both studies employed histological analysis to investigate tissue-damage. This paper exclusively concentrates on studying the area of tissue-damage or cracks resulting from coated needle insertion because tissue-damage is directly related to mechanical trauma, inflammatory response, and hemorrhage [13,27-32]. To conduct a histological study on tissue-damage caused by needle insertion, various sequential steps are followed, including sample collection, fixation, processing, staining, and microscopic examination [5,6,26,32]. In this research, bovine kidney tissues were used to study the tissue-damage caused by both coated and uncoated needles.

2. Materials and methods

In this study, two types of needles, stainless steel needles without any coating and with coating of the PDA-PTFE-AC, were analyzed. The needles with a 1.27 mm diameter and a trocar tip were used throughout the experiments. The coating procedure involves first coating the needles with PDA by immersing them in a PDA solution for the entire day. Afterward, the needles are coated with PTFE-AC using the dip coating method and then cured (sintered) at 373°C. A custom test setup was utilized for the measurement of insertion force (Fig. 1). The setup comprised several components, including a linear motor actuator (Velmex, Inc., NY, USA), a force sensor (Nano17® ATI Industrial Automation, Apex, NC, USA, resolution: 1/160 N, maximum range: 17 N), a needle holder connected to the force sensor, and a tissue holder. Additionally, the test setup incorporated a data acquisition system (DAQ) to read the force sensor data and transfer it to the computer. The procedure involved the needle being inserted at a velocity of 5 mm per second, to a maximum depth of 3.5 cm. The force sensor began measuring the data as soon as the needle pierced the tissue. The force measurement was programmed using LabVIEW software utilizing the DAQ system. The insertion depth of 3.5 cm was controlled by the linear actuator motor controller via COSMOS software (Velmex, Inc., NY, USA), where the insertion velocity (5 mm/s) and distance to travel (3.5 cm) were specified. Five insertions in the central part of the kidney lobe were performed, with each set consisting of three uncoated needles and three coated needles. The central part of the kidney lobe is a reasonable insertion location to minimize the effect of tissue heterogeneity since the variation in tissue stiffness within each layer is minimal. The coating method and experimental setup utilized in this study are in alignment with the procedures outlined in our prior publication [18].

Subsequently, a histological study was carried out to examine the tissue-damage induced by inserting both coated and uncoated needles.

The histological process can be expressed in the subsequent flow chart, as shown in Fig. 2. Three samples, each containing an insertion hole, were extracted from the kidney. Subsequently, each sample was dissected to dimensions of $2 \times 2 \times 1$ cm³ and then individually housed in cassettes (Fig. 2a). The dissection of the bovine kidney is performed with the scalpel. The dissected tissue samples with the cassette were placed in a plastic container with 10 % formalin for the fixation process (Fig. 2b). This process prevents decay and retains tissue structural integrity, ensuring it can be examined without significant degradation. The tissue samples were soaked in the formalin solution for 48 h before being transferred to 70 % isopropyl alcohol to remove any remaining water. After dehydration and clearing, the tissue samples were embedded in paraffin wax for proper infiltration (Fig. 2c). Next, a microtome was employed to section the tissue samples, cutting thin sections of 5 μm (Fig. 2d). These 5 µm sections were then affixed to glass slides and readied for the subsequent staining process.

The histological staining procedure followed standard protocols, utilizing the steps outlined in research papers published by Sahlabadi [5] and Gidde [6]. To achieve the desired Hematoxylin and Eosin stain, ethanol solutions of varying concentrations were prepared and poured into Tissue-Tek station dishes. The slides were sequentially dehydrated in pure xylene and a 50 % xylene - 50 % ethanol mixed solution for five minutes each. They were then stained with 1 % hematoxylin and 1 % eosin Y, followed by double rinsing with deionized water. The procedures were replicated in reverse for rehydration, immersing slides in alcohol concentrations from 100 % to 70 %. The staining procedure concluded with a final five-minute immersion in pure xylene. After staining, slides were left to air dry for ten minutes before 100 µL of Permount was applied. Then, coverslips were placed, and excess Permount and air bubbles were removed with manual hand pressure. Slides were then left to air dry for a day prior to microscopic examination. Stained slides samples are shown in Fig. 2e. An Olympus GX-71 inverted microscope with an attached Olympus U-TVO.5XC color camera was utilized to visualize and capture stained slide images at a magnification range of 5X [5,6,32] (Fig. 2f). Next, the tissue-damage area analysis for both coated and uncoated needles was performed using the ImageJ software. To make the selection of the tissue-damage area easier, images were converted to 8-bit grayscale, and the software was calibrated using a reference line of 250 µm. Then, using the WAND tool, the irregular damage area was measured. Here, the WAND tool assists in selecting the area by tracing the light-colored region in the microscopic images. After selecting the light-colored region, the imageJ software MEASURE tool was used to calculate the area.

3. Results and discussion

The force-depth curves in Fig. 3 exhibit a nonlinear hyperplastic behavior typical of kidney soft tissue, but due to the heterogeneous

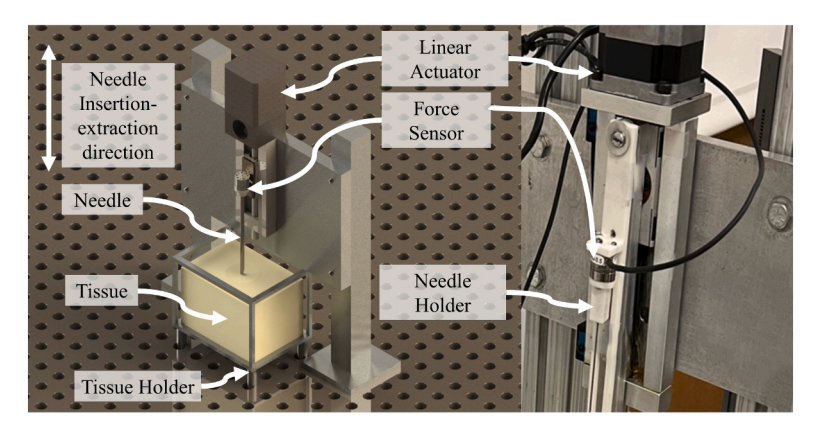


Fig. 1. Experimental setup for measuring needle insertion force.

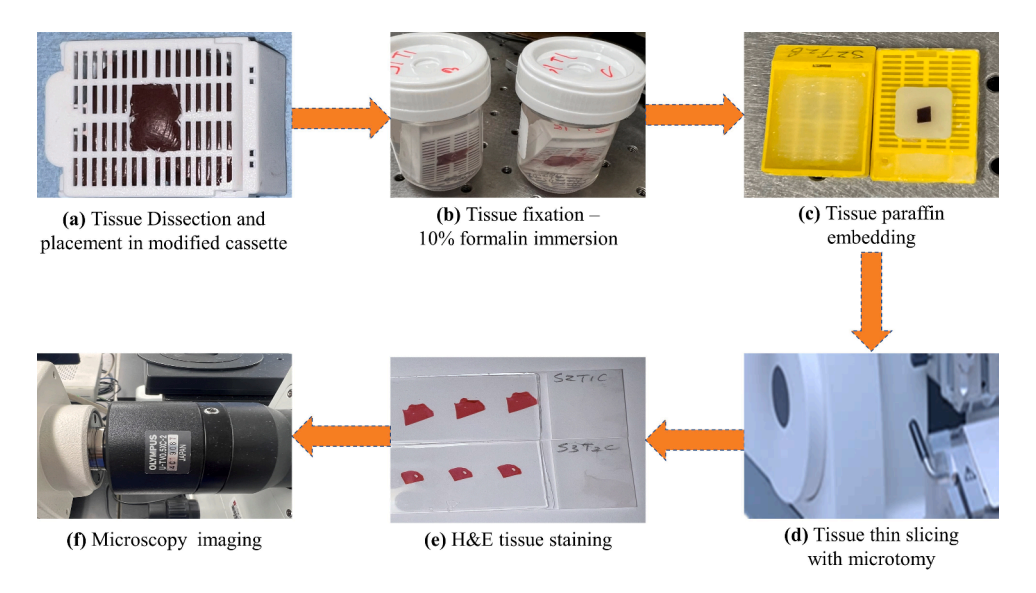


Fig. 2. Histological procedure flow chart: (a) Tissue Dissection and placement in Modified cassette, (b) Tissue fixation -10 % formalin immersion, (c) Tissue Paraffin embedding, (d) Tissue thing slicing with microtomy, (e) H&E tissue staining, (f) Microscopy imaging.

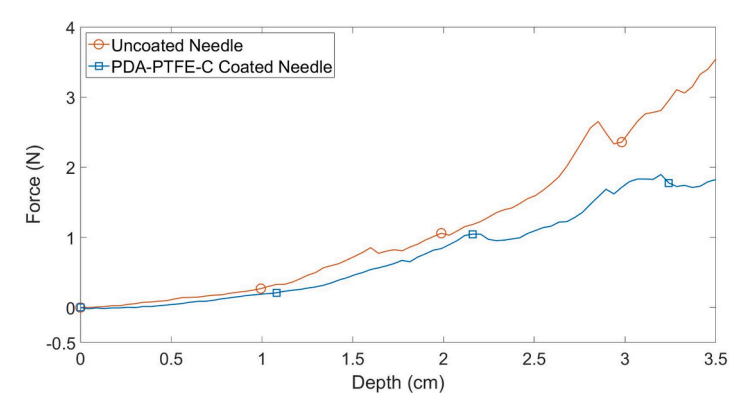


Fig. 3. Average needle insertion force of 15 experiments using uncoated needle and 15 experiments using coated needle in the bovine kidney tissue. The range of uncoated needle standard deviation (SD) is 0.0021N < SD < 0.4043 N and the range of coated needle standard deviation is 0.0105N < SD < 0.3829 N.

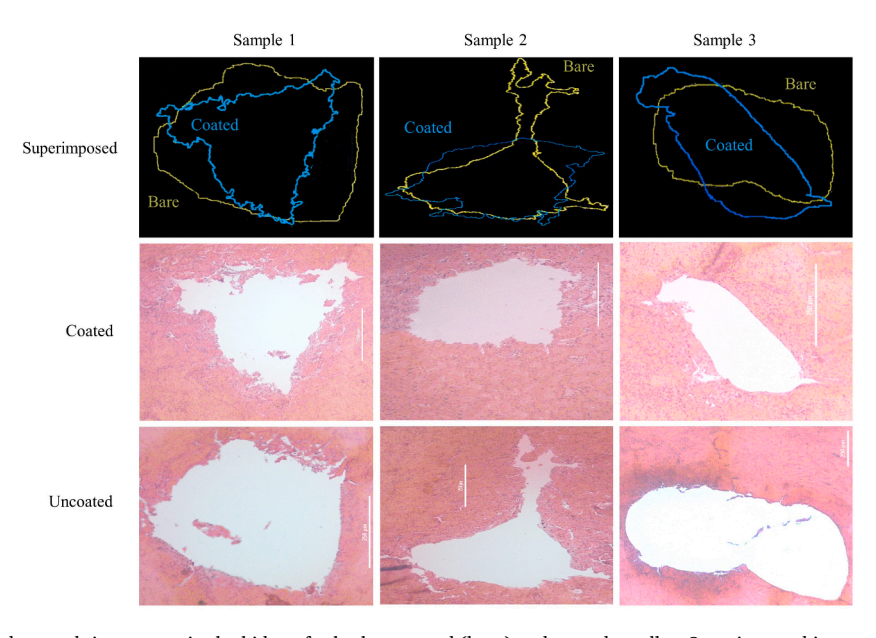


Fig. 4. Microscopic images of damaged tissue areas in the kidney for both uncoated (bare) and coated needles. Superimposed images are included for reference and do not originate from the same insertion location.

nature of bovine kidney tissue. The presented insertion force data is the mean taken from five needle insertion tests performed for each type of needle. The insertion force involving coated needles demonstrated a significant decrease in force compared to uncoated needles. For all experiments, a needle was inserted from the top of the kidney lobe to ensure uniform conditions for each type of needle insertion comparison. The location of needle insertion was determined by the needle insertion hole, and the area of bovine kidney tissue in that vicinity was immediately sectioned to identify any tissue damage/cracks and facilitate the histological procedure. Upon analysis of the insertion force data from this study, the force exerted by uncoated needles is greater than that of the PDA-PTFE-AC coated needles. The uncoated needles demonstrated a mean maximum insertion force of 3.54±0.052 N, whereas the coated needles exhibited a lower mean maximum insertion force of 1.82 ± 0.023 N. A two-tailed t-test was conducted, resulting in p-values of 0.0010 for insertion forces. The p-values have demonstrated statistical significance by rejecting the null hypothesis, confirming a significant difference in the insertion forces between the coated and uncoated needles. Coating the needles with PDA-PTFE-AC helped in reducing the average maximum insertion force by 49 %.

Next, bovine kidney tissue samples were analyzed using H&E staining and observed through an Olympus GX-71 microscope at 5X magnification. In order to ensure accurate measurements, the microscope was calibrated using a micrometer calibration slide. Fig. 4 presents a series of microscopic images depicting bovine kidney tissue samples. The images showcase the tissue-damage areas, which are highlighted by distinct light-colored regions. The superimposed images are a comparison between the uncoated and coated needle tissue-damage areas. Visually, the superimposed images show that the coated needle has less tissue-damage areas than the uncoated needle. This is also evaluated by quantifying the damaged area numerically in the next paragraph.

Table 1 shows the tissue-damaged area for each sample separately and a mean of it with the standard deviation. The mean tissue-damage caused by the uncoated needle was found to be $0.201\pm0.063~\text{mm}^2,$ while the coated needle resulted in $0.121\pm0.067~\text{mm}^2$ in bovine kidney tissue. According to the results of the two-tailed t-test, the data strongly rejects the null hypothesis, as evidenced by the extremely low p-value of 0.01. This significant p-value demonstrates a statistically significant difference in tissue-damage area between the uncoated and coated needles.

The hypothesis proposing that a decrease in insertion force is associated with a reduction in tissue-damage has been substantiated and confirmed through this study. The histological process was immediately carried out after the needle extraction from the tissue to prevent tissue shrinkage. After removing the needle, the tissue tends to partially regain its original shape, making it difficult to locate the precise insertion path. Furthermore, it is important to consider that the formalin fixation process and the paraffin-embedded sample sectioning process can also influence tissue-damage. Nevertheless, considering that each tissue sample was equally affected, it is feasible to compare the extent of the damaged areas. The PDA-PTFE-AC coated needle induced notably less tissue-damage during the needle insertion processes, amounting to an average of 39 % reduction in tissue-damage during the procedure.

Sahlabadi [4,5] and Gidde [6] developed a bioinspired needle aimed at reducing the insertion force, a development that consequently helps to reduce tissue-damage - a finding they discovered through a histological study. Many researchers who have employed various coatings on needles have not explored their potential impact on tissue-damage. Therefore, it was essential to investigate tissue-damage in relation to PDA-PTFE-AC coated needles, to explore the hypothesis that a reduction in insertion force also results in decreased tissue-damage. This novel research demonstrates that the PDA-PTFE-AC coated needle not only reduces the insertion force, but it also minimizes tissue-damage for the composite coated needles insertion in bovine kidneys due to the low-friction coating on the needle.

Table 1
Tissue-damaged area of uncoated and coated needles in (mm²).

	Damaged Area (mm ²)		Mean damaged Area (mm²)	
	Uncoated Needle	Coated Needle	Uncoated Needle	Coated Needle
Sample 1 Sample 2	0.288 0.176	0.217 0.079	0.201 ± 0.063	0.121 ± 0.067
Sample 3	0.139	0.069		

4. Conclusions

The findings of this study confirm that the composite-coated needle with PDA-PTFE-AC reduces insertion force and minimizes tissue-damage. In comparison to uncoated needles, this composite-coated needle can decrease the average insertion force by 49 %. Moreover, histological analysis further corroborates this conclusion, demonstrating a 39 % average reduction in tissue-damage with coated needles. This implies that reducing tissue-damage could reduce the risks associated with needle insertion. Nevertheless, additional research and testing are necessary to elevate this study to a clinical level, ensuring the durability and safety of the needle coating.

Declarations

The following additional information is required for submission. Please note that this form runs over two pages and failure to respond to these questions/statements will mean your submission will be returned to you. If you have nothing to declare in any of these categories then this should be stated.

Ethical approval

Work on human beings that is submitted to Medical Engineering & Physics should comply with the principles laid down in the Declaration of Helsinki; Recommendations guiding physicians in biomedical research involving human subjects. Adopted by the 18th World Medical Assembly, Helsinki, Finland, June 1964, amended by the 29th World Medical Assembly, Tokyo, Japan, October 1975, the 35th World Medical Assembly, Venice, Italy, October 1983, and the 41st World Medical Assembly, Hong Kong, September 1989. You should include information as to whether the work has been approved by the appropriate ethical committees related to the institution(s) in which it was performed and that subjects gave informed consent to the work.

Author contribution

Kavi Patel and Parsaoran Hutapea have contributed to the planning, designing, and executing of the experiments. Additionally, they work together in manuscript writing, along with the editing of grammar and spelling.

Declaration of Competing Interest

All authors must disclose any financial and personal relationships with other people or organisations that could inappropriately influence (bias) their work. Examples of potential conflicts of interest include employment, consultancies, stock ownership, honoraria, paid expert testimony, patent applications/registrations, and grants or other funding.

Acknowledgements

Authors thank the Penn Center Musculoskeletal Disorders Histology Core (P30-AR069619) for their assistance with the histological analysis. This work was supported by the National Science Foundation under grant CMMI Award #1917711.

References

- [1] Eriksson M, Reichardt P, Sundby Hall K, et al. Needle biopsy through the abdominal wall for the diagnosis of gastrointestinal stromal tumour - Does it increase the risk for tumour cell seeding and recurrence? Eur J Cancer 2016;59: 128–33. doi: 10.1016/j.ejca.2016.02.021.
- [2] Parker SH, Stavros AT, Dennis MA. Needle biopsy techniques. Radiol Clin North Am 1995;33:1171–86. https://doi.org/10.1016/S0033-8389(22)00651-0.
- [3] Chargari C, Deutsch E, Blanchard P, et al. Brachytherapy: an overview for clinicians. CA Cancer J Clin 2019;69:386–401. https://doi.org/10.3322/ casc 21578
- [4] Sahlabadi M, Hutapea P. Tissue deformation and insertion force of bee-stinger inspired surgical needles. ASME. J. Med. Devices 2018;12(3):034501. https://doi. org/10.1115/1.4040637
- [5] Sahlabadi M, Gidde STR, Gehret P, et al. Histological evaluation of tissue damage caused by bioinspired needle insertion. Adv Biomater Devices Med 2018;5:1–6. http://abiodem.com/download/files/abiodem 2018 no1 p1 sahlabadi.pdf.
- [6] Gidde STR, Acharya SR, Kandel S, et al. Assessment of tissue damage from mosquito-inspired surgical needle. Minim Invasive Ther Allied Technol 2022;31: 1112–21. https://doi.org/10.1080/13645706.2022.2051718.
- [7] Yang C, Xie Y, Liu S, et al. Force modeling, identification, and feedback control of robot-assisted needle insertion: a survey of the literature. Sensors 2018;18(2):561. https://doi.org/10.3390/s18020561.
- [8] Abolhassani N, Patel R, Moallem M. Control of soft tissue deformation during robotic needle insertion. Minim. Invasive Ther. Allied Technol. 2009;15:165–76. https://doi.org/10.1080/13645700600771645.
- [9] Adams SB, Moore GE, Elrashidy M, et al. Effect of needle size and type, reuse of needles, insertion speed, and removal of hair on contamination of joints with tissue debris and hair after arthrocentesis. Vet Surg 2010;39:667–73. https://doi.org/ 10.1111/j.1532-950X.2010.00649.x.
- [10] O'Leary MD, Simone C, Washio T, et al. Robotic needle insertion: effects of friction and needle geometry. In: IEEE International Conference on Robotics and Automation. 2. Taipei, Taiwan. New York: IEEE; 2003. p. 1774–80. https://doi. org/10.1109/ROBOT.2003.1241851. Sept. 14-19.
- [11] Sahlabadi M, Hutapea P. Novel design of honeybee-inspired needles for percutaneous procedure. Bioinspir Biomim 2018;13:036013. https://doi.org/ 10.1088/1748-3190/aaa348.
- [12] Scali M, Pusch TP, Breedveld P, et al. Ovipositor-inspired steerable needle: design and preliminary experimental evaluation. Bioinspir Biomim 2017;13:016006. https://doi.org/10.1088/1748-3190/aa92b9.
- [13] Casanova F, Carney PR, Sarntinoranont M. In vivo evaluation of needle force and friction stress during insertion at varying insertion speed into the brain. J Neurosci Methods 2014;237:79–89. https://doi.org/10.1016/j.jneumeth.2014.08.012.
- [14] McClung WL, Daniel SC, McGregor W, et al. Enhancing needle durability by silicone coating of surgical needles. J Emerg Med 1995;13:515–8. https://doi.org/ 10.1016/0736-4679(95)80010-7
- [15] Dearnaley G, Arps JH. Biomedical applications of diamond-like carbon (DLC) coatings: a review. Surf Coatings Technol 2005;200:2518–24. https://doi.org/ 10.1016/j.surfcoat.2005.07.077.

- [16] Chu JP, Jang JSC, Huang JC, et al. Thin film metallic glasses: unique properties and potential applications. Thin Solid Films 2012;520:5097–122. https://doi.org/ 10.1016/j.tsf.2012.03.092.
- [17] Foust SA. Ultrathin ptfe coating for hypodermic needles enabled by musselinspired pda adhesive layer [master's thesis]. Fayetteville (AR): University of Arkansas; 2014.
- [18] Patel KI, Zhu L, Ren F, et al. Effect of composite coating on insertion mechanics of needle structure in soft materials. Med Eng Phys 2021;95:104–10. https://doi.org/ 10.1016/j.medengphy.2021.07.008.
- [19] Gidde STR, Islam S, Kim A, et al. Experimental study of mosquito-inspired needle to minimize insertion force and tissue deformation. J. Med. Eng 2022;237:113–23. https://doi.org/10.1177/09544119221137133.
- [20] Aziz NA, Mohamed M, Mohamad M, et al. Influence Of Activated Carbon Filler On The Mechanical Properties Of Wood Composites. ARPN J. Eng. Appl. Sci. 2015;10: 376–86.
- [21] Brooks JK, Bashirelahi N, Reynolds MA. Charcoal and charcoal-based dentifrices: a literature review. J Am Dent Assoc 2017;148:661–70. https://doi.org/10.1016/j. adaj.2017.05.001.
- [22] Sanchez N, Fayne R, Burroway B. Charcoal: an ancient material with a new face. Clin Dermatol 2020;38:262–4. https://doi.org/10.1016/j. clindermatol 2019 07 025
- [23] Silberman J, Galuska MA, Taylor A. Activated Charcoal. StatPearls Publishing; 2023. https://www.ncbi.nlm.nih.gov/books/NBK482294/.
- [24] Iguchi S, Yamaguchi N, Takami H, et al. Higher efficacy of direct hemoperfusion using coated activated-charcoal column for disopyramide poisoning: a case report. Med (Baltimore) 2017;96. https://doi.org/10.1097/md.0000000000008755. Epub ahead of print 1 December.
- [25] Aktaş Ö, Çeçen F. Bioregeneration of activated carbon: a review. Int Biodeterior Biodegradation 2007;59:257–72. https://doi.org/10.1016/j.ibiod.2007.01.003.
- [26] Alturkistani HA, Tashkandi FM, Mohammedsaleh ZM. Histological stains: a literature review and case study. Glob J Health Sci 2015;8:72–9. https://doi.org/ 10.5539/gibs.v8n3n72.
- [27] Casanova F, Carney PR, Sarntinoranont M. Effect of needle insertion speed on tissue injury, stress, and backflow distribution for convection-enhanced delivery in the rat brain. PLoS ONE 2014;9:e94919. https://doi.org/10.1371/journal. pone.0094919.
- [28] Barua R, Das S, Roy Chowdhury A, et al. Experimental and simulation investigation of surgical needle insertion into soft tissue mimic biomaterial for minimally invasive surgery. Proc Inst Mech Eng H 2023;237:254–64. https://doi.org/ 10.1177/09544119221143860.
- [29] Usach I, Martinez R, Festini T, et al. Subcutaneous injection of drugs: literature review of factors influencing pain sensation at the injection site. Adv Ther 2019;36: 2986–96. https://doi.org/10.1007/s12325-019-01101-6.
- [30] Tsumura R, Takishita Y, Iwata H. Needle insertion control method for minimizing both deflection and tissue damage. J. Med. Robot. Res 2019;04:1842005. https:// doi.org/10.1142/S2424905×18420059.
- [31] Tsumura R, Takishita Y, Fukushima Y, et al. Histological evaluation of tissue damage caused by rotational needle insertion. In: 38th Annual International Conference of the IEEE Engineering in Medicine and Biology Society (EMBC). Orlando, FL, USA, New York: IEEE; 2016. p. 5120–3. https://doi.org/10.1109/ embc.2016.7591879. Aug. 16-20.
- [32] Slaoui M, Fiette L. Histopathology procedures: from tissue sampling to histopathological evaluation. Methods Mol Biol 2011;691:69–82. https://doi.org/ 10.1007/978-1-60761-849-2-4.